

# Synthesis and Properties of Polythiophene Derivatives Containing Triphenylamine Moiety and Their Photovoltaic Applications

YAOWEN LI, LILI XUE, HAIJIAN XIA, BIN XU, SHANPENG WEN, WENJING TIAN

State Key Laboratory of Supramolecular Structure and Materials, Jilin University, Changchun 130012, People's Republic of China

Received 22 January 2008; accepted 6 March 2008

DOI: 10.1002/pola.22737

Published online in Wiley InterScience (www.interscience.wiley.com).

**ABSTRACT:** A series of novel soluble polythiophene derivatives containing triphenylamine moiety were synthesized by Grignard metathesis (GRIM) method. The structures of the polymers were characterized and their physical properties were investigated. High molecular weight ( $M_n$  up to 25,800 g/mol) and thermostable polymers were obtained. The absorption spectra demonstrated that the absorption wavelength of the polymers could be tuned dramatically by introducing thiophene units in the main chain of the polymers. Photoluminescence spectra indicated that there was intramolecular energy transfer from the side chain to the main chain, and the maximum emission was red-shifted gradually with the increase of thiophene units in the main chain. Cyclic voltammetry displayed that the polymers possessed relatively high oxidation potential, which promised good air stability and high open circuit voltage for photovoltaic cells application. Finally, bulk heterojunction photovoltaic devices were fabricated by using the polymers as donors and (6,6)-phenyl C<sub>61</sub>-butyric acid methyl ester (PCBM) as acceptor. The maximal open circuit voltage of the photovoltaic cells reached 0.71–0.87 V and the power conversion efficiencies of the devices were measured between 0.014% and 0.45% under white light at 100 mW/cm<sup>2</sup>. © 2008 Wiley Periodicals, Inc. *J Polym Sci Part A: Polym Chem* 46: 3970–3984, 2008

**Keywords:** copolymerization; conjugated polymers; UV-vis spectroscopy; electrochemistry

## INTRODUCTION

In the past few decades, conjugated polymers with an extended  $\pi$ -conjugation have received considerable attention due to their electronic and photonic applications, such as light-emitting diodes,<sup>1,2</sup> photovoltaic cells (PVCs),<sup>3,4</sup> and thin film transistors.<sup>5,6</sup> Polythiophenes (PTs) are the most promising conjugated polymers because of their relatively high charge carrier mobility and long wavelength absorption in comparison with

other conjugated polymers.<sup>7</sup> For example, regioregular poly(3-hexylthiophene) (P3HT) have exhibited excellent properties in PVCs.<sup>8,9</sup> However, P3HT only absorbs a part of the visible light and exhibits the relatively low open-circuit voltage ( $V_{oc}$ ).<sup>10</sup> To further improve the related properties and explore the full potential applications of these materials, chemical modifications of PTs have been performed actively. One successful strategy to achieve broader absorption of PTs is based on the pioneering work by Li and coworkers.<sup>11,12</sup> They synthesized PTs with conjugated bi(thienylenevinylene) as side chain and made the absorption band in the region from 350 to 650 nm, resulting in a good power conver-

Correspondence to: W. Tian (E-mail: wjtian@jlu.edu.cn)

*Journal of Polymer Science: Part A: Polymer Chemistry*, Vol. 46, 3970–3984 (2008)  
© 2008 Wiley Periodicals, Inc.

sion efficiency (PCE) of 3.18%. PTs with substituents other than alkyl groups have also been investigated, among which those with electron-donating alkoxy groups have displayed promising optical properties.<sup>13</sup> However, these PTs show relatively low  $V_{oc}$  because of the relative high the highest occupied molecular orbital (HOMO) level, so as to limit the PCE of the device.

Actually, the PCE of polymer photovoltaic devices is determined by three main factors: the efficiency of exciton generation, the efficiency of exciton dissociation into free charge carriers, and the efficiency of their unhindered collection by the electrodes. To increase the device efficiency, the active layer should absorb as many of the incident photons as possible to generate a maximum of excitons,<sup>14,15</sup> therefore, low band gap polymers are necessary since the absorption of the active layer should match the solar spectrum well. The factors that influence the band-gap of a polymer are conjugated length, solid-state ordering, and the presence of electron-withdrawing or -donating moieties. The effective conjugated length, which is dependent upon the torsion angle between the repeating units along the polymer backbone, can be controlled by choosing sterically hindered units along the polymer back-chain or by introducing bulky side-chains to twist the units out of plane.<sup>16,17</sup> While, the  $V_{oc}$  of a PVCs based on polymer and (6,6)-phenyl  $C_{61}$ -butyric acid methyl ester (PCBM) blend system is determined by the difference between the HOMO of the polymer and lowest unoccupied molecular orbital (LUMO) of PCBM.<sup>18,19</sup> Therefore, the HOMO level is also an important parameter to be considered when designing a new electron-donating polymer.

Triphenylamine (TPA) is a preferred electron-donating moiety with excellent hole transporting properties and their derivatives have been widely investigated for almost two decades.<sup>20,21</sup> Owing to the noncoplanarity of the three phenyl substituents, TPA derivatives can be viewed as 3D systems and the amorphous character of these materials offers possibilities to develop active materials for PVCs with isotropic optical and charge-transport properties.<sup>22</sup> Recently, Roncali, J. and coworkers synthesized various series of star-shaped molecules based on TPA small molecules with combinations of thienylenevinylene conjugated branches and electron-withdrawing indanedione or dicyanovinyl groups, which have been applied to organic

PVCs as donor materials and got PCE of 1.20%.<sup>23</sup> To our knowledge, the application of TPA-based polymers for photovoltaic devices has been scarcely considered.

Herein, we report the synthesis and photovoltaic properties of a series of new conjugated PT derivatives: poly((E)-*N,N*-diphenyl-4-(2-(thiophen-3-yl)vinyl)aniline)P3T-TPA, poly((E)-4-(dodecyloxy)-*N*-(4-(dodecyloxy)phenyl)-*N*-(4-(2-(thiophen-3-yl)vinyl)phenyl)aniline) P3T-DDTPA, and copolymers poly((E)-4-(dodecyloxy)-*N*-(4-(dodecyloxy)phenyl)-*N*-(4-(2-(thiophen-3-yl)vinyl)phenyl) aniline-*co*-3-hexylthiophene) P1–P4. The introduction of sterically hindered units TPA through a vinylene bridge enhances the hole transporting property, the effective conjugated length, the intramolecular energy transfer from side chain to main chain, and high air-stability of the polymers. To improve the solubility of the synthesized polymers, alkoxy chains were introduced to TPA. The incorporation of 3-hexylthiophene (HT) units onto the conjugated mainchain increased the conjugated length and lowered the band gap. The UV–vis absorption suggested that the introduction of HT units in the main chain of the polymers could induce the red-shift and broad absorption. The Photoluminescence (PL) spectra showed that significant intramolecular energy transfer behavior between the side chain and main chain. The electrochemical properties indicated that these polymers had relative high air-stability. Furthermore, the properties of the PVCs based on bulk heterojunction architecture demonstrated that these polymers could be good candidates for the PVCs.

## EXPERIMENTAL

### Materials

Methylmagnesium bromide, 3-bromothiophene, *t*-BuOK, Ni(dppp)Cl<sub>2</sub>, and triphenylamine were purchased from Acros. 3-Methylthiophene, 1-bromododecane, NBS, phosphorous acid triethyl ester, POCl<sub>3</sub>, and all the other solvents were purchased from Beijing Chemical Reagent. THF and aether were distilled over sodium, and DMF was dried by distillation over CaH<sub>2</sub>. 2,5-Dibromo-3-hexylthiophene was prepared from 3-bromothiophene according to literature procedures.<sup>24,25</sup>

### Measurement

The infrared spectroscopy spectra were recorded via the KBr pellet method by using a Nicolet

Impact 410 FTIR spectrophotometer. The elemental analysis was carried out with a Thermoquest CHNS-Ovelemental analyzer. The gel permeation chromatographic (GPC) analysis was carried out with a Waters 410 instrument with tetrahydrofuran as the eluent (flow rate: 1 mL/min, at 35 °C) and polystyrene as the standard. The mass spectra were recorded on a Kratos MALDITOF mass system, and the spectrum was recorded in the linear mode with anthracene-1,8,9-triol as the matrices. The thermogravimetric analysis (TGA) was performed on a Perkin Elmer Pyris 1 analyzer under nitrogen atmosphere (100 mL/min) at a heating rate of 10 °C/min. <sup>1</sup>H and <sup>13</sup>C NMR spectra were measured using a Bruker AVANCE-500 NMR spectrometer spectrometer and a Varian Mercury-300 NMR, respectively. UV-visible absorption spectra were measured using a Shimadzu UV-3100 spectrophotometer. The photoluminescence spectra of spin-cast films and solution were measured with a RF-5301PC spectrofluorophotometer. Electrochemical measurements of these derivatives were performed with a Bioanalytical Systems BAS 100 B/W electrochemical workstation. Atomic force microscopy (AFM) images of blend films were carried out using a Nanoscope IIIa Dimension 3100. Current-voltage characteristics of the PVCs in the dark and under illumination of 100 mW/cm<sup>2</sup> white light from a xenon lamp (Jobin Yvon, FL-1039) were measured on computer-controlled Keithley 2400 Source Meter measurement system.

## Synthesis

### 2,5-Dibromo-3-methylthiophene (1)

3-Methylthiophene (2.52 g, 15 mmol) was dissolved in THF (15 mL). *N*-Bromosuccinimide (5.34 g, 30 mmol) was added to the solution over a period of 5 min. The solution was stirred at room temperature for 2 h. The solvent was removed *in vacuo* and hexane (50 mL) was added (to precipitate all the succinimide). The mixture was filtered through a silica plug (to remove the succinimide) and the solvent was removed *in vacuo*. Distillation under vacuum gave 2.35 g (9.2 mmol, yield 61.3%) as a colorless oil.

<sup>1</sup>H NMR (500 MHz, CDCl<sub>3</sub>, TMS): δ (ppm) 6.769 (s, 1H, —Th), 2.148 (s, 3H, —CH<sub>3</sub>). ELEM. ANAL. CALCD. for C<sub>5</sub>H<sub>4</sub>Br<sub>2</sub>S: C, 23.46; H, 1.58; Found: C, 23.42; H, 1.61.

### 2,5-Dibromo-3-bromomethyl Thiophene (2)

Compound **1** (2.56 g, 10 mmol) and *N*-bromosuccinimide (1.78 g, 10 mmol) were put in a flask with CCl<sub>4</sub> (20 mL). Then a small amount of benzoyl peroxide was added as an initiator. The mixture was refluxed for 3 h. The completion of the reaction was indicated by the appearance of succinimide on the surface of the solution. The organic layer was washed with water and dried over anhydrous MgSO<sub>4</sub>. Distillation under vacuum gave 2.65 g (7.9 mmol, yield 79%) as a colorless oil.

<sup>1</sup>H NMR (500 MHz, CDCl<sub>3</sub>, TMS): δ (ppm) 6.999 (s, 1H, —Th), 4.365 (s, 2H, —CH<sub>2</sub>). ELEM. ANAL. CALCD. for C<sub>5</sub>H<sub>3</sub>Br<sub>3</sub>S: C, 17.93; H, 0.9; Found: C, 17.90; H, 0.98.

### 2,5-Dibromothiophen-3-ylmethyl Phosphonic Acid Diethyl Ester (3)

Compound **3** (3.35 g, 10 mmol) and phosphorous acid triethyl ester (6.64 g, 40 mmol) were put in a flask and heated to 160 °C for 2 h. Then it was removed the excessive phosphorous acid triethyl ester under vacuum. The crude product was purified by column chromatography on silica gel with ethyl acetate:petroleumether (2:5) as the eluant to give red brown oil 3.25 g (8.3 mmol, 83%).

<sup>1</sup>H NMR (500 MHz, CDCl<sub>3</sub>, TMS): δ (ppm) 7.016 (s, 1H), 4.085 (m, 4H, —OCH<sub>2</sub>—), 3.112 (d, 2H, *J* = 21 Hz, —CH<sub>2</sub>), 1.298 (t, 6H, *J* = 7 Hz, —CH<sub>3</sub>). ELEM. ANAL. CALCD. for C<sub>9</sub>H<sub>13</sub>Br<sub>2</sub>O<sub>3</sub>PS: C, 27.57; H, 3.34; Found: C, 27.50; H, 3.30.

### 4-Diphenylaminobenzaldehyde (4)

DMF (2 mL, 24 mmol) was put into a 50-mL flask, kept in ice-water, and then phosphorous oxychloride (1.1 mL, 12 mmol) was added dropwise to the stirred DMF. After 20 min, TPA (0.98 g, 4 mmol) was added into the mixture with stirring at 60 °C for 2 h. After cooling, the solution was poured into cold water. The resulting mixture was neutralized to pH 7 with 2 M NaOH aqueous solution and extracted with chloroform. The extract was washed with plenty of water and NaCl, successively. The organic extracts were dried over anhydrous MgSO<sub>4</sub>, evaporated and purified with column chromatography on silica gel with ethyl acetate : petroleumether (1:10) as the eluant to give yellow solid 0.93 g (3.4 mmol, yeild 85%).

$^1\text{H}$  NMR (500 MHz,  $\text{CDCl}_3$ , TMS):  $\delta$  (ppm) 9.812 (s, 1H,  $-\text{CHO}$ ), 7.677 (d, 2H,  $J = 9$  Hz,  $-\text{Ph}$ ), 7.341 (t, 4H,  $J = 8$  Hz,  $-\text{Ph}$ ), 7.155–7.182 (m, 6H,  $-\text{Ph}$ ), 7.016 (d, 2H,  $J = 8.5$  Hz,  $-\text{Ph}$ ). ELEM. ANAL. CALCD. for  $\text{C}_{19}\text{H}_{15}\text{NO}$ : C, 83.49; H, 5.53; N, 5.12; Found: C, 83.45; H, 5.47; N, 5.20.

**(E)-4-(2-(2,5-Dibromothiophen-3-yl)vinyl)-N,N-diphenylaniline (5)**

Compounds **3** (0.90 g, 2.3 mmol) and **4** (0.57 g, 2.1 mmol) were dissolved in 35 mL of fresh dried THF, then *t*-BuOK (0.28 g, 2.5 mmol) was added into the mixture under  $\text{N}_2$  atmosphere quickly and refluxed for 24 h. The reaction mixture was cooled to room temperature, then water and chloroform were added successively. The two phases were separated, and the water phase was extracted twice with chloroform. The combined organic extracts were washed three times with water, dried over anhydrous  $\text{MgSO}_4$ , evaporated under vacuum, and purified with column chromatography on silica gel with ethyl acetate:petroleumether (1:50) as the eluant to give yellow solid (0.59 g, 54.5%).

FTIR (KBr,  $\text{cm}^{-1}$ ): 952 (trans,  $\text{CH}=\text{CH}$ ).  $^1\text{H}$  NMR (500 MHz,  $\text{CDCl}_3$ , TMS):  $\delta$  (ppm) 7.360 (d, 2H,  $J = 8.5$  Hz,  $-\text{Ph}$ ), 7.254–7.284 (t, 4H,  $J = 7.5$  Hz,  $-\text{Ph}$ ), 7.204 (s, 1H,  $-\text{Th}$ ), 7.114 (d, 4H,  $J = 8$  Hz,  $-\text{Ph}$ ), 7.048 (t, 4H,  $J = 7.25$  Hz,  $-\text{Ph}$ ), 6.879 (d, 1H,  $J = 16.0$  Hz,  $-\text{vinylic}$ ), 6.838 (d, 1H,  $J = 16.5$  Hz,  $-\text{vinylic}$ ),  $^{13}\text{C}$  NMR (75 MHz,  $\text{CDCl}_3$ , TMS):  $\delta$  (ppm) 147.871, 147.339, 139.371, 130.811, 130.431, 129.306, 127.466, 127.329, 124.653, 123.239, 123.163, 118.236, 111.731, 109.220. MALDI-TOF-MS calcd. for  $\text{C}_{24}\text{H}_{17}\text{Br}_2\text{NS}$ : 511.27; Found: 510.9.

**1-(Dodecyloxy)-4-iodobenzene (6)**

To a stirred mixture of 4-iodophenol (14.5 g, 65.89 mmol), 1-bromododecane (17.4 mL, 72.59 mmol), and DMF (100 mL) under  $\text{N}_2$  was added  $\text{K}_2\text{CO}_3$  (18.2 g, 132.0 mmol). The reaction mixture was refluxed for 15 h, then cooled to room temperature and filtered. Most of solvent was removed *in vacuo*. The obtained oil was dissolved in chloroform, washed with water, dried over anhydrous  $\text{MgSO}_4$  evaporated, and purified with column chromatography on silica gel with ethyl acetate:petroleumether (1:10) as the eluant to colorless oil 24.3 g (62.58 mmol, 94.8%).

$^1\text{H}$  NMR (500 MHz,  $\text{CDCl}_3$ , TMS):  $\delta$  (ppm) 7.539 (d, 2H,  $J = 8.5$  Hz,  $-\text{Ph}$ ), 6.673 (d, 2H,  $J =$

8.5 Hz,  $-\text{Ph}$ ), 3.908 (t, 2H,  $J = 6.5$  Hz,  $-\text{OCH}_2$ ), 1.763 (m, 2H,  $-\text{CH}_2$ ), 1.434 (m, 2H,  $-\text{CH}_2$ ), 1.26–1.35 (m, 16H,  $-\text{CH}_2$ ), 0.884 (t, 3H,  $J = 7.0$  Hz,  $-\text{CH}_3$ ). ELEM. ANAL. CALCD. for  $\text{C}_{18}\text{H}_{29}\text{IO}$ : C, 55.67; H, 7.53; Found: C, 55.62; H, 7.60.

**Bis(4-(dodecyloxy)phenyl)amino-benzene (7)**

The mixture of **6** (24.30 g, 62.58 mmol), phenylamine (2.60 mL, 26 mmol),  $\text{K}_2\text{CO}_3$  (28.0 g, 208 mmol),  $1 \mu\text{Cu}$  (6.50 g, 80 mmol), 18-crown-6 (1.85 g, 7 mmol), and *o*-dichlorobenzene (100 mL) were refluxed under  $\text{N}_2$  atmosphere, after  $\sim 20$  h the reaction mixture was filtered hot through a fritted funnel with celite and washed with dichloromethane. The dichloromethane was then washed several times with water, dried over anhydrous  $\text{MgSO}_4$  evaporated, and purified with column chromatography on silica gel with ethyl acetate:petroleumether (1:50) as the eluant to white powder 6.7 g (11 mmol, 42.0%).

$^1\text{H}$  NMR (500 MHz,  $\text{CDCl}_3$ , TMS):  $\delta$  (ppm) 6.793–7.157 (m, 13H,  $-\text{Ar}$ ), 3.916 (br, 4H,  $-\text{OCH}_2$ ), 1.763 (m, 4H,  $-\text{CH}_2$ ), 1.445 (m,  $-\text{CH}_2$ , 4H), 1.264–1.357 (m,  $-\text{CH}_2$ , 32H), 0.880 (t, 6H,  $J = 6.75$  Hz,  $-\text{CH}_3$ ). ELEM. ANAL. CALCD. for  $\text{C}_{42}\text{H}_{63}\text{NO}_2$ : C, 82.16; H, 10.34; N, 2.28; Found: C, 82.01; H, 10.31; N, 2.36.

**4-Bis(4-(dodecyloxy)phenyl)amino-benzaldehyde (8)**

Compound **8** was synthesized according to the procedure described for **4** using **7** (7.00 g, 11.40 mmol), phosphorous oxychloride (6.86 mL, 68.40 mmol), and DMF (10.50 mL, 136.80 mmol). A yellowish solid was obtained in 82% yield (6.03 g, 9.35 mmol).

$^1\text{H}$  NMR (500 MHz,  $\text{CDCl}_3$ , TMS):  $\delta$  (ppm) 9.750 (s, 1H,  $-\text{CHO}$ ), 9.618 (d, 2H,  $J = 8.5$  Hz,  $-\text{Ph}$ ), 7.110 (d, 4H,  $J = 9.0$  Hz,  $-\text{Ph}$ ), 6.873 (d, 4H,  $J = 8.5$  Hz,  $-\text{Ph}$ ), 6.839 (d, 2H,  $J = 9.0$  Hz,  $-\text{Ph}$ ), 3.941 (t, 4H,  $J = 6.5$  Hz,  $-\text{OCH}_2$ ), 1.780 (m, 4H,  $-\text{CH}_2$ ), 1.454 (m, 4H,  $-\text{CH}_2$ ), 1.266–1.350 (m, 32H,  $-\text{CH}_2$ ), 0.881 (t, 6H,  $J = 7.0$  Hz,  $-\text{CH}_3$ ). ELEM. ANAL. CALCD. for  $\text{C}_{43}\text{H}_{63}\text{NO}_3$ : C, 80.45; H, 9.89; N, 2.18; Found: C, 80.39; H, 9.91; N, 2.15.

**(E)-4-(2-(2,5-Dibromothiophen-3-yl)vinyl)-N,N-bis(4-(dodecyloxy)phenyl)aniline (9)**

Compound **9** was synthesized according to the procedure described for **5** using **8** (0.60 g, 0.93 mmol), **3** (0.44 g, 1.12 mmol), THF 30 mL, *t*-



BuOK (0.13 g, 1.13 mmol). Yellowish oil was obtained in 71.6% yield (0.59 g, 0.69 mmol).

FTIR (KBr,  $\text{cm}^{-1}$ ): 958 (trans, CH=CH).  $^1\text{H}$  NMR ( $\text{CDCl}_3$ ):  $\delta$  (ppm) 7.28–7.29 (d, 2H, –Ar), 7.19 (s, 1H, –Ar), 7.04–7.05 (d, 4H, –Ar), 6.87–6.88 (d, 2H, –Ar), 6.81–6.83 (d, 6H, –Ar and –vinylic), 3.93 (t, 4H,  $J = 5.75$  Hz,  $-\text{OCH}_2$ ), 1.77 (m, 4H,  $-\text{CH}_2$ ), 1.451 (m, 4H,  $-\text{CH}_2$ ), 1.27–1.36 (m, 32 H,  $-\text{CH}_2$ ), 0.88 (t, 6H,  $J = 7.0$  Hz,  $-\text{CH}_3$ ).  $^{13}\text{C}$  NMR (75 MHz,  $\text{CDCl}_3$ , TMS):  $\delta$  (ppm) 155.702, 148.920, 140.268, 139.615, 131.130, 128.348, 127.359, 126.781, 119.939, 117.172, 115.286, 111.592, 108.642, 68.257, 31.917, 29.667, 29.636, 29.606, 29.408, 29.347, 26.078, 22.687, 14.112. MALDI-TOF-MS calcd. for  $\text{C}_{48}\text{H}_{65}\text{Br}_2\text{NO}_2\text{S}$ : 879.91; Found: 880.1.

### General Procedure for Polymerization

The polymer P3T-TPA, P3T-DDTPA, and copolymer P1–P4 was synthesized via condensation polymerization using the Grignard metathesis (GRIM) method initially reported by McCullough and coworkers.<sup>26,27</sup>

### Synthesis of P3T-TPA and P3T-DDTPA

The two polymers were prepared by the same method. Monomer **5** (0.15 g, 0.3 mmol) or **9** (0.26 g, 0.3 mmol) was dissolved in 10 mL of dry THF under  $\text{N}_2$  atmosphere. Methylmagnesium bromide (0.32 mL, 1.0 M solution in THF) was added and the mixture was heated to reflux for 1 h. Then  $\text{Ni}(\text{dppp})\text{Cl}_2$  (3 mg) was added and the solution was stirred at reflux for 2 h. The mixture was poured into 100 mL of methanol and filtered into a Soxhlet thimble. Soxhlet extrac-

tions were performed with methanol, hexane and chloroform. The chloroform fraction was reduced and dried *in vacuo* to afford 41 and 34%, respectively.

**P3T-TPA.**  $^1\text{H}$  NMR ( $\text{CDCl}_3$ ):  $\delta$  (ppm) 7.32–7.44 (br, 2H, –Ar), 7.15–7.30 (br, 5H, –Ar and Th), 6.81–7.10 (br, 10H, –Ph). ELEM. ANAL. CALCD. for  $\text{C}_{24}\text{H}_{17}\text{NS}$ : C, 82.05; H, 4.80; N, 3.99; Found: C, 80.39; H, 4.13; N, 3.45.

**P3T-DDTPA.**  $^1\text{H}$  NMR ( $\text{CDCl}_3$ ):  $\delta$  (ppm) 7.31–7.43 (br, 2H, –Ar), 7.19 (br, 1H, –Ar), 7.04 (br, 4H, –Ar), 6.89–6.90 (br, 2H, –Ar), 6.80 (br, 6H, –Ar and vinylic), 3.90 (br, 4H,  $-\text{OCH}_2$ ), 1.76 (br, 4H,  $-\text{CH}_2$ ), 1.43 (br, 4H,  $-\text{CH}_2$ ), 1.26 (br, 32H,  $-\text{CH}_2$ ), 0.87 (br, 6H,  $-\text{CH}_3$ ). ELEM. ANAL. CALCD. for  $\text{C}_{48}\text{H}_{65}\text{NO}_2\text{S}$ : C, 79.89; H, 9.02; N, 1.94; found: C, 76.10; H, 7.73; N, 2.10.

### Synthesis of P1–P4

These polymers were synthesized with procedure reported by Pei and coworkers.<sup>13</sup> Monomer **9** and 2,5-dibromo-3-hexylthiophene were dissolved in dry THF with different amount to modulate the ratio of  $n:m$  under  $\text{N}_2$  atmosphere and the ratio was listed in Table 1. Methylmagnesium bromide (1.0 M solution in THF) according to the amount of compound **9** and 2,5-dibromo-3-hexylthiophene was added and the mixture was heated to reflux for 1 h. Then the corresponding  $\text{Ni}(\text{dppp})\text{Cl}_2$  (1 mol %) was added. After 3 h, the mixture was poured into 100 mL of methanol and filtered. The solid was redissolved in chloroform and filtered then deposited with methanol for several times, collected by fil-

**Table 1.** Molecular Weights, Thermal Properties, and Composition of the Polymers

	$M_n^a (\times 10^4)$	$M_w/M_n^a$	TGA <sup>b</sup> (°C)	Comonomer Feed Molar Ratio <sup>c</sup>	Comonomer Molar Ratio in Copolymers <sup>c,d</sup>
P3T-TPA	1.08	1.69	299	–	–
P3T-DDTPA	1.45	1.40	188	1:0	1:0
P1	0.63	1.07	247	1:1	10:1
P2	0.67	1.10	283	1:2	2:1
P3	0.82	1.29	274	1:4	1:1
P4	2.58	1.47	383	1:6	1:4.8

<sup>a</sup> Calculated from GPC (eluent: THF; polystyrene standards).

<sup>b</sup> Temperature at 5% weight loss by a heating rate of 10 °C/min under nitrogen.

<sup>c</sup> Comonomer ratios are monomer **9** to 3-hexylthiophene in P1–P4.

<sup>d</sup> Calculated from  $^1\text{H}$  NMR spectra based on relative abundances of the  $-\text{OCH}_2-$  and  $-\text{CH}_2-$  groups adjoining the TPA and thiophene, respectively.

tration and dried *in vacuo* to afford 30–54% yields.

**P1 (Monomer 9-co-3-Hexylthiophene with 10:1).** The actual molar ratio of monomer **9** and 2,5-dibromo-3-hexylthiophene is 1:1. Yield: (33%).  $^1\text{H}$  NMR ( $\text{CDCl}_3$ ):  $\delta$  (ppm) 7.27–7.35 (br, 2H, —Ar), 7.13–7.19 (br, 1H, —Th), 7.04 (br, 4H, —Ar), 6.88 (br,  $\sim$  2.0H, —Ar), 6.81 (br, 6H, —Ar), 3.93 (br, 4H, — $\text{CH}_2$ ), 2.81 (br, 0.20H, Th— $\text{CH}_2$ ), 1.77 (br,  $\sim$  4H), 1.45 (br,  $\sim$  4H), 1.27 (br,  $\sim$  32H), 0.88 (br,  $\sim$  6H). ELEM. ANAL. CALCD.: C, 79.63; H, 9.01; N, 1.90; Found: C, 77.04; H, 8.30; N, 1.76.

**P2 (Monomer 9-co-3-hexylthiophene with 2:1).** The actual molar ratio of monomer **9** and 2,5-dibromo-3-hexylthiophene is 1:2. Yield: (30%).  $^1\text{H}$  NMR ( $\text{CDCl}_3$ ):  $\delta$  (ppm) 7.29–7.35 (br, 2H, —Ar), 7.13–7.19 (br, 1H, —Th), 7.04 (br,  $\sim$  4.5H, 3-hexylthiophene-H and —ArH), 6.88 (br, 2.0H), 6.81 (br, 6H), 3.92 (br, 4H, — $\text{OCH}_2$ ), 2.80 (br, 1H, Th— $\text{CH}_2$ ), 1.77 (br,  $\sim$  5H, dialkoxy and alkyl), 1.44 (br,  $\sim$  5H, dialkoxy and alkyl), 1.27 (br,  $\sim$  34H, dialkoxy and alkyl), 0.88 (br,  $\sim$  8H, dialkoxy and alkyl). ELEM. ANAL. CALCD.: C, 79.30; H, 8.98; N, 1.75; Found: C, 76.46; H, 7.20; N, 1.60.

**P3 (Monomer 9-co-3-hexylthiophene with 1:1).** The actual molar ratio of monomer **9** and 2,5-dibromo-3-hexylthiophene is 1:4. Yield: (38%).  $^1\text{H}$  NMR ( $\text{CDCl}_3$ ):  $\delta$  (ppm) 7.32–7.43 (br, —Ar, 2H), 7.12–7.19 (br, —Th, 1H), 6.99–7.04 (br, 5H, 3-hexylthiophene—H and Ar—H), 6.87–6.9 (br, —Ar, 2.0H), 6.81 (br, —Ar, 6H), 3.91 (br, 4H, — $\text{OCH}_2$ ), 2.80 (br, 2H, thiophene— $\text{CH}_2$ —), 1.77 (br,  $\sim$  6H, dialkoxy and alkyl), 1.44 (br,  $\sim$  6H, dialkoxy and alkyl), 1.27 (br,  $\sim$  36H, dialkoxy and alkyl), 0.88 (br,  $\sim$  9H, dialkoxy and alkyl). ELEM. ANAL. CALCD.: C, 78.64; H, 8.93; N, 1.58; Found: C, 75.17; H, 7.76; N, 1.72.

**P4 (Monomer 9-co-3-hexylthiophene with 1:4.8).** The actual molar ratio of monomer **9** and 2,5-dibromo-3-hexylthiophene is 1:6. Yield: (54%).  $^1\text{H}$  NMR ( $\text{CDCl}_3$ ):  $\delta$  (ppm) 7.32–7.35 (br, 2H, —Ar), 7.05–7.12 (br, 5H, —Th and —Ar), 6.98 (s, 5H, 3-hexylthiophene-H), 6.9–6.92 (br, 2.0H, —Ar), 6.81 (br, 6H, —Ar), 3.92 (br, 4H, — $\text{OCH}_2$ ), 2.80 (br, 9.6H, thiophene— $\text{CH}_2$ ), 1.71 (br,  $\sim$  14H, dialkoxy and alkyl), 1.44 (br,  $\sim$  14H, dialkoxy and alkyl), 1.35 (br,  $\sim$  20H, alkyl), 1.26 (br,  $\sim$  32H, dialkoxy), 0.87–0.91 (br,  $\sim$  21H, dialkoxy and alkyl). ELEM.

ANAL. CALCD.: C, 76.00; H, 8.72; N, 0.92; Found: C, 74.42; H, 7.25; N, 1.26.

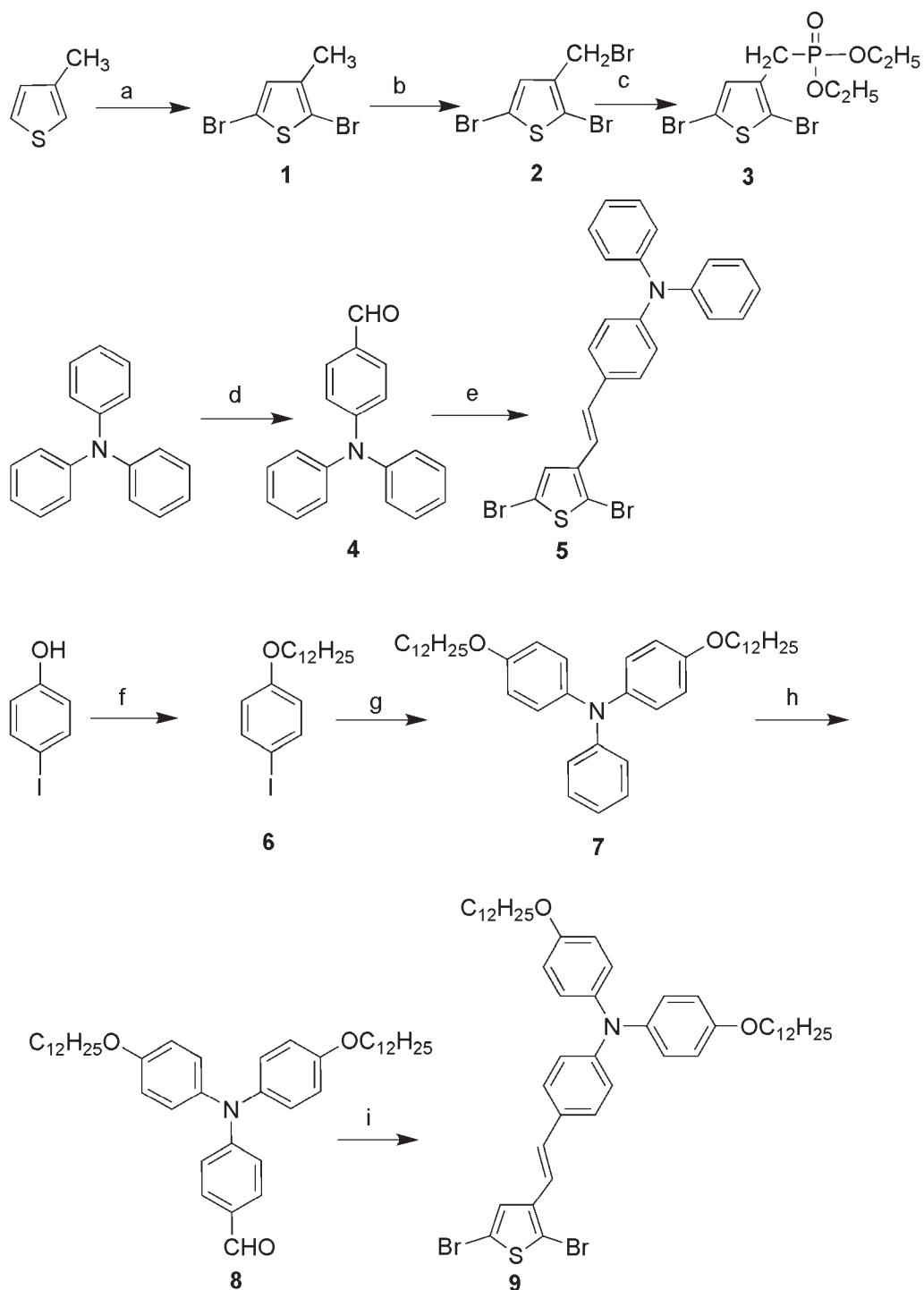
### Photovoltaic Device Fabrication and Characterization

For device fabrication, The ITO glass was pre-cleaned and modified by a thin layer of PEDOT:PSS, which was spin-cast from a PEDOT:PSS aqueous solution (H. C. Starck) on the ITO substrate, and the thickness of the PEDOT:PSS layer is about 50 nm. The active layer was prepared from a 1:1 by weight solution (10 mg/mL) in chlorobenzene of the respective polymer as electron donor and PCBM as electron acceptor. After spin-coating the blend from solution at 1000 rpm, the devices were completed by evaporating a 0.6 nm LiF layer protected by 100 nm of Al at a base pressure of  $5 \times 10^{-4}$  Pa. The effective photovoltaic area as defined by the geometrical overlap between the bottom ITO electrode and the top cathode was 4 or 5 mm<sup>2</sup>. The thickness of the photoactive layer was  $\sim$  100 nm, measured by the Ambios Technology XP-2 in the dark and under illumination of 100 mW/cm<sup>2</sup> white light from a xenon lamp (Jobin Yvon, FL-1039) were measured on computer-controlled Keithley 2400 Source Meter measurement system. Current–voltage characteristics of the solar cells in the dark and under illumination of 100 mW/cm<sup>2</sup> white light from a Xenon lamp (Jobin Yvon, FL-1039) were measured on computer-controlled Keithley 2400 SourceMeter measurement system. All the measurements were performed under ambient atmosphere at room temperature.

## RESULTS AND DISCUSSION

### Synthesis and Characterization

The synthesis of the monomers is outlined in Scheme 1. The first key intermediate monomer **5** was obtained by the Wittig–Horner reaction,<sup>28</sup> which was realized by refluxing the 4-diphenylaminobenzaldehyde and compound **3**. Another key intermediate monomer **9** was prepared in several facile reactions: The alkylation of 4-iodophenol with 1-bromododecane in the presence of  $\text{K}_2\text{CO}_3$  gave **6**, which was then converted to **7** according to the Ullmann condensation reaction.<sup>29</sup> The monomer **8** was obtained by the Vielsmier reaction,<sup>30</sup> and the intermediate



**Scheme 1.** Synthesis of monomers. Reagents and conditions: (a) NBS, THF, 2 h; (b) NBS, BPO, CCl<sub>4</sub>, reflux, 3 h; (c) P(OC<sub>2</sub>H<sub>5</sub>)<sub>3</sub>, 160 °C, 2 h; (d) POCl<sub>3</sub>, DMF, 60 °C, 2 h; (e) monomer 2, t-BuOK, dried THF, N<sub>2</sub> atmosphere, 24 h; (f) 1-bromododecane, K<sub>2</sub>CO<sub>3</sub>, DMF, N<sub>2</sub> atmosphere, 15 h; (g) K<sub>2</sub>CO<sub>3</sub>, 1 $\mu$ Cu, 18-crown-6, o-dichlorobenzene, reflux, N<sub>2</sub> atmosphere, 20 h; (h) POCl<sub>3</sub>, DMF, 90 °C, 2 h; (i) monomer 3, t-BuOK, dried THF, N<sub>2</sub> atmosphere, 24 h.





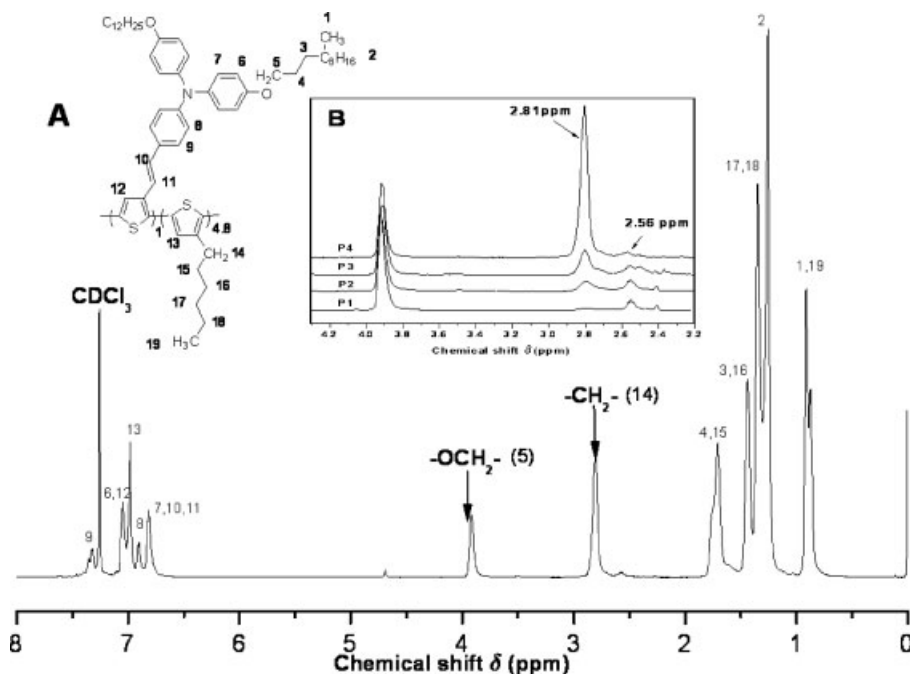


**Figure 1.** (A)  $^1\text{H}$  NMR spectrum and chemical structure of P4 in  $\text{CDCl}_3$  solution; (B)  $^1\text{H}$  NMR spectrum of P1–P4 for the determination of relatively regioregularity.

synthesized by using methylmagnesium–bromine exchange reaction and  $\text{Ni}(\text{dppp})\text{Cl}_2$  as catalyst, which leads to high regioselectivity in polymers. Usually, the regioregularity of poly(3-alkylthiophene)s and poly(3-arylthiophene)s can be estimated by comparing the  $^1\text{H}$  NMR peaks of the proton on the 4-position of the thiophene ring or the  $^1\text{H}$  NMR peaks of the protons of  $-\text{CH}_2-$  group on the side chain close to the phenyl ring. However, it's hard to estimate regioregularity by comparing the  $^1\text{H}$  NMR peaks of the proton on the 4-position of the thiophene ring for the two homopolymers, because the  $^1\text{H}$  NMR peaks of the thiophene ring is too close to the proton on the side chain to distinguish them. Besides, the protons of the  $-\text{OCH}_2-$  group on the side chain are far from the main chain, the regioregular coupling might have little influence on the  $^1\text{H}$  NMR spectrum. Thus, it is incredible to determine the regioregularity of this kind of conjugated side chain PTs by the  $^1\text{H}$  NMR signal of the protons of  $-\text{OCH}_2-$  group.<sup>32</sup> The four random copolymers P1–P4 were also obtained via GRIM reaction. The values of  $n:m$  (ratio of comonomer) were modulated by controlling the feed ratio of the monomer **9** and 2,5-dibromo-3-hexylthiophene (monomer **10**). The actual  $n:m$  values were determined by the relative area of the peaks at 3.92 ppm (the

$-\text{OCH}_2-$  groups adjoining the TPA) and 2.81 ppm ( $\alpha$ -methylene attached directly to the thiophene rings) from  $^1\text{H}$  NMR spectra of the copolymers (as shown in Fig. 1 and Table 1). Notably, the calculated  $n:m$  values are much higher than the feed ratios, which indicates that during the GRIM copolymerization, the monomer **9** is more reactive and easier to add onto the propagating polymer chain than the monomer **10**. The process of polymerization catalyzed by  $\text{Ni}(\text{dppp})\text{Cl}_2$  is determined by an oxidative addition step, and for the growing copolymers, the selective oxidative addition is more likely to occur at the thiophene of the more highly conjugated intermediates. Therefore, the monomer **9** which containing trans vinylene and conjugated moiety of TPA as side chain is more reactive than monomer **10** containing an alkyl side chain.<sup>33,34</sup> From the  $^1\text{H}$  NMR spectra, we found that the peak at 2.81 ppm is  $\alpha$ -methylene proton's peak of HT units, while the minor peak at 2.56 ppm is the sum of peaks due to  $\alpha$  and  $\beta$ -methylene protons which are subject to varying degrees of coupling<sup>35</sup> (see Fig. 1). In other words, the peak at 2.56 ppm is caused by the different environment of  $\alpha$ -methylene protons, which suggests the degree of disorder structure for the copolymers.<sup>36</sup> Therefore, the relative region-regularity of the copolymers can be esti-

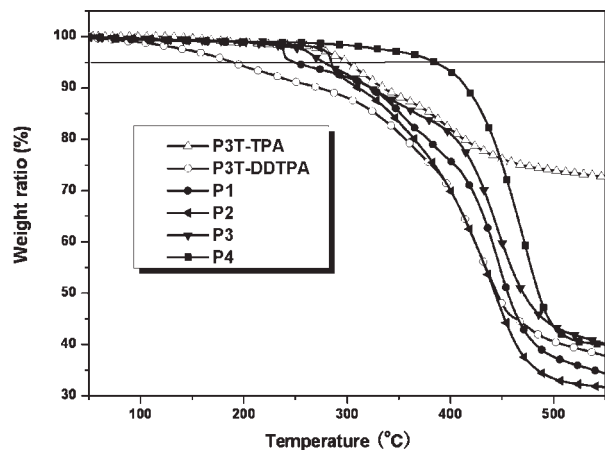


**Figure 2.** TGA thermograms of the polymers.

mated from  $^1\text{H}$  NMR spectra. The four copolymers (P1–P4) exhibit irregularity of different extent due to the effect of the steric hindrance side chains on the random copolymerization. With the increase of HT units the intensity of the peak at 2.56 ppm is getting weaker and weaker, which indicates that the copolymers display higher regioregularity.

The average molecular weights of polymers were determined by GPC with polystyrene as standards. P3T-TPA, P3T-DDTPA, and P4 has a relative high molecular weight ( $M_n > 10$  kg/mol), whereas the  $M_n$  of P1, P2, P3 are only 6.2–8.3 kg/mol. The steric hindrance side chain (TPA), which prevented the copolymerization between comonomer **9** and HT units, should be the main reason for the low polymerization. The narrow molecular weight distribution with the polydispersity index ( $M_w/M_n$ ) ranging from 1.07 to 1.69 indicated that P1–P4 are copolymers rather than the blends of two homopolymers. TGA of the polymers shown in Figure 2 proved that these polymers had good thermal stabilities. The physical properties of the polymers are summarized in Table 1.

### Optical Properties

Figure 3 shows the normalized UV-vis absorption spectra of P3T-TPA, P3T-DDTPA, and P1–P4 in chloroform solution and thin films on quartz substrates. For comparison, P3HT is also shown in solution and thin film. All the polymers show two maximum absorption peaks in dilute solution except P3HT. The one in visible region is attributed to  $\pi$ - $\pi^*$  transition of the conjugated polymer main chains, while the one in the UV region is

attributed to the conjugated side chains (TPA moiety). Obviously, for the copolymers, the relative intensity between the peak in visible region and the peak in UV region is getting stronger with the increase of thiophene units in the main chain. Comparing the absorption spectrum of P3T-TPA and P3T-DDTPA in dilute solution, we found that P3T-DDTPA had a broader peak in the visible absorption compared to P3T-TPA resulting from the introduction of the dialkoxy-substituted TPA. In addition, the largest red-shift of the maximum absorption in visible region is only 14 nm from P1 to P3 and the maximum absorption becomes broader (in the range of 440–500 nm) because of the increased conjugated length. And as expected, with the continuous increase of thiophene, the absorption of P4 has nearly 30 nm red-shift and becomes much broader. The absorption spectra in thin film are

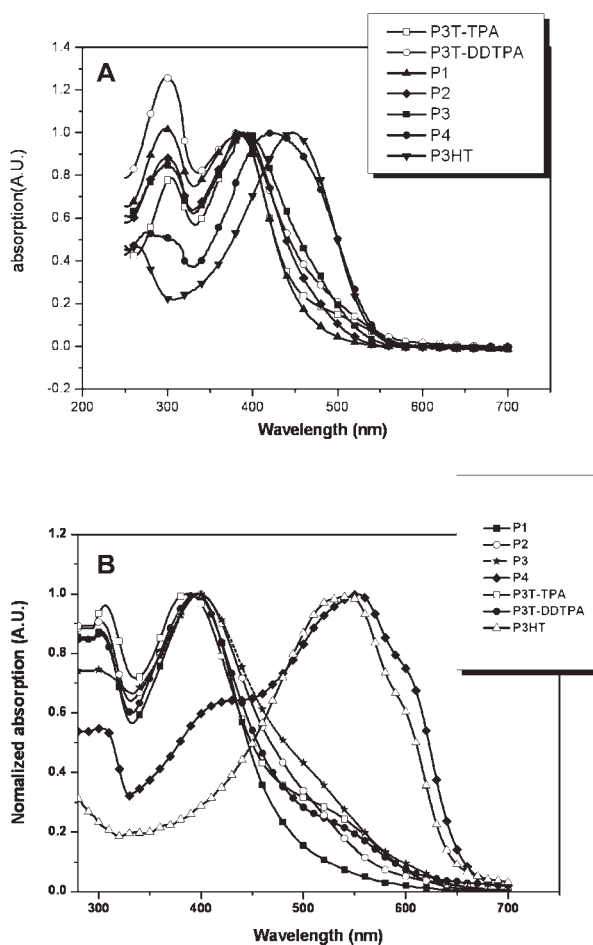


**Figure 3.** Normalized absorption spectra of the polymer (A) in chloroform solutions with the concentration of  $10^{-5}$  mol/mL; (B) films spin-coated from chloroform solution.

**Table 2.** Optical and Electrochemical Properties of the Polymers

Polymer	In Solution		In Film	$E_{\text{Ox}}^{\text{onset}}$ (V)/HOMO (eV)	$E_{\text{Red}}^{\text{onset}}$ (V)/LUMO (eV)	Electrochem. $E_{\text{g,ec}}$ (eV)	Optical $E_{\text{g,opt}}$ (eV) <sup>c</sup>
	$\lambda_{\text{max}}^{\text{abs}}$ (nm) <sup>a</sup>	$\lambda_{\text{max}}^{\text{em}}$ (nm) <sup>a</sup>	$\lambda_{\text{max}}^{\text{abs}}$ (nm) <sup>b</sup>				
P3T-TPA	386/304	430/576	386/306	0.51/−5.17	−1.72/−2.94	2.23	2.50
P3T-DDTPA	383/299	488	395/302	0.43/−5.09	−1.69/−2.97	2.12	2.60
P1	383/297	516	397/302	0.54/−5.20	−1.72/−2.94	2.26	2.54
P2	389/299	532	398/302	0.52/−5.18	−1.70/−2.96	2.22	2.26
P3	386/300	560	397/301	0.51/−5.17	−1.65/−3.01	2.16	2.03
P4	423/298	576	552/301	0.41/−5.07	−1.74/−2.92	2.15	2.03

<sup>a</sup>  $1 \times 10^{-5}$  M in anhydrous chloroform, wavelength of two maximum absorbances.

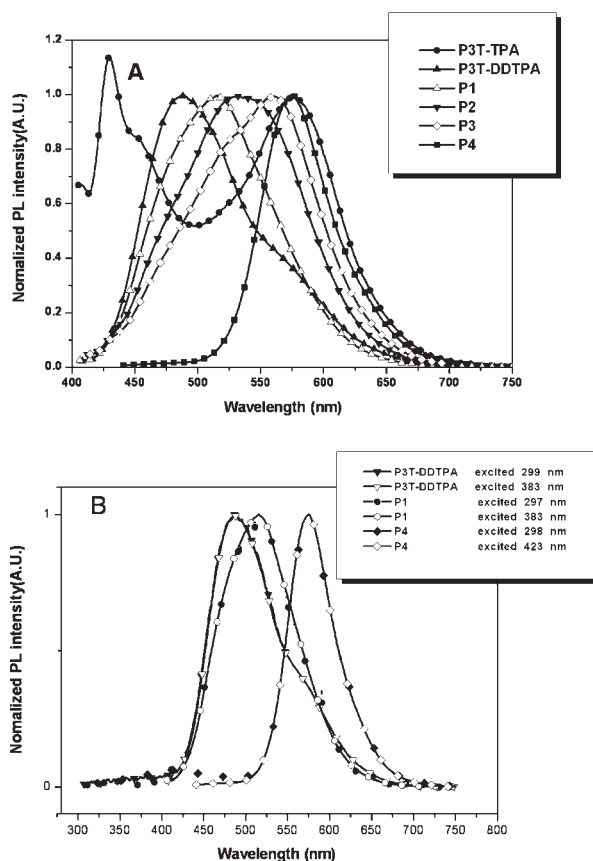
<sup>b</sup> Films cast on quartz substrates.

<sup>c</sup> The optical band gap ( $E_{\text{g,opt}}$ ) was obtained from absorption edge.

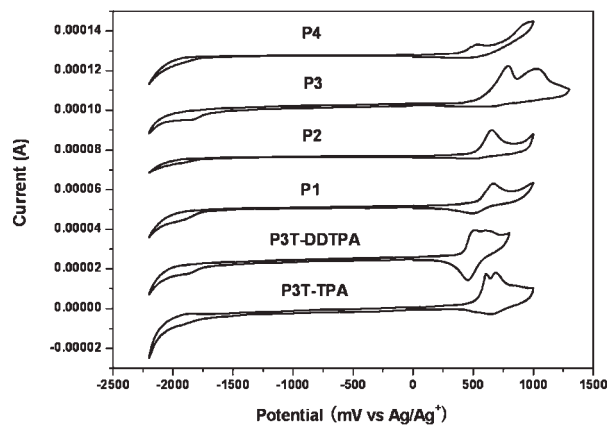
generally similar to those in dilute solutions for the polymers except P4. The small shifts (1–14 nm) of the absorption peak in the visible region between the dilute solution and solid-state suggests that these polymers have similar conformations in both states due to the incorporation of sterically hindered chain (TPA moiety), which indicates that the TPA moiety decreases the aggregated configuration formed in solid state. However, in the case of P4, the large shift (129 nm) between the absorption in solution and film can be explained by the presence of large numbers of thiophene units in the main chain, which plays an important role in the formation of aggregated configuration in solid state. The absorption data of polymers are summarized in Table 2.

Figure 4(a) shows the PL spectra of the polymers in chloroform solution. The P3T-TPA has two emission peaks, which probably originate from the emission of side chain and main chain, respectively. However, P3T-DDTPA exhibited only one emission peak, because the electron-donating ability of the large dialkoxy-substituted TPA moiety enhances the conjugated length and leads to the energy transfer from side chains to main chains via vinylene bridge. The similar results are also obtained for P1–P4. On the other hand, energy transfer can be further proved by the PL spectra of P3T-DDTPA, P1, and P4 in dilute solution, excited at the two wavelengths corresponding to the maximal absorption peaks. For example, when P3T-DDTPA was excited at 299 and 383 nm, as shown in Figure 4(b), the PL spectra of the polymers were almost the same, which indicates that there is an intramolecular energy transfer of the excitons from the conjugated side chain to the main chain.<sup>11,37</sup> The PL maxima from P3T-DDTPA to P1–P4 are red-shifted gradually with the increase of HT units,

due to the formation of the higher extended  $\pi$ -delocalized system. The PL spectra data of polymers are also summarized in Table 2.



**Figure 4.** (A) Normalized PL spectra of the polymer in chloroform solutions excited at maximal absorption of visible region with the concentration of  $10^{-5}$  mol/mL; (B) normalized PL spectra of P3T-DDTPA, P1, and P4 excited at the two maximal absorption peaks of UV and visible regions in chloroform solution, respectively, with  $10^{-5}$  mol/mL.



**Figure 5.** Cyclic voltammograms of P3T-TPA, P3T-DDTPA, P1–P4 films on platinum electrode in 0.1 mol/L  $\text{Bu}_4\text{NClO}_4$  in  $\text{CH}_3\text{CN}$  solution, at a scan rate of  $100 \text{ mV S}^{-1}$ .

### Electrochemical Properties

Figure 5 shows the cyclic voltammograms of the polymers using  $\text{Bu}_4\text{NClO}_4$  as supporting electrolyte in acetonitrile solution with platinum button working electrodes, a platinum wire counter electrode and an  $\text{Ag}/\text{AgNO}_3$  reference electrode under the  $\text{N}_2$  atmosphere. Ferrocene was used as the internal standard. All the polymers show reversible or partly reversible redox behavior, which was attributed to the high electrical activity. The onset oxidation potential ( $E_{\text{Ox}}^{\text{onset}}$ ) of all the polymers are observed in the range of 0.41–0.54 V compared to the  $E_{\text{Ox}}^{\text{onset}}$  of P3HT (0.348 V)<sup>13</sup> indicates that they have relative higher air-stability than P3HT. The redox potential of  $\text{Fc}/\text{Fc}^+$  (which has an absolute energy level of  $-4.8 \text{ eV}$  relative to the vacuum level for calibration<sup>38,39</sup>) is located at 0.14 V in 0.1 M  $\text{Bu}_4\text{NClO}_4/\text{acetonitrile}$  solution. So the evaluation of HOMO and LUMO levels as well as the band gap ( $E_{g,ec}$ ) could be done according to the following equations:

$$\text{HOMO}(\text{eV}) = -E_{\text{Ox}}^{\text{onset}} - 4.66$$

$$\text{LUMO}(\text{eV}) = -E_{\text{Red}}^{\text{onset}} - 4.66$$

$$E_{g,ec}(\text{eV}) = E_{\text{Ox}}^{\text{onset}} - E_{\text{Red}}^{\text{onset}}$$

where  $E_{\text{Ox}}^{\text{onset}}$  and  $E_{\text{Red}}^{\text{onset}}$  are the measured potentials relative to  $\text{Ag}/\text{Ag}^+$ . The electrochemical properties as well as the energy level parameters of polymers are listed in Table 2.

From Table 2 it can be seen that the HOMO energy level decreases proportionally with the increase of the conjugated length of the copolymer, except in the case of P3T-DDTPA. This behavior is in good agreement with the observations of Barbarella et al.<sup>40</sup> Because the HOMO level of the donor polymer and the LUMO of the acceptor in a heterojunction PVC determined the  $V_{\text{oc}}$  of a PVC, the relatively low HOMO level ( $-5.07$  to  $-5.20 \text{ eV}$ ) of the synthesized polymers compared with other PT derivatives, for example, P3HT (HOMO =  $-4.75 \text{ eV}$ ),<sup>13</sup> POT-co-DOT (HOMO =  $-4.55 \text{ eV}$ ),<sup>13</sup> and biTV-PTs (HOMO =  $-4.93$  to  $-4.96 \text{ eV}$ ),<sup>12</sup> may be favored for the improvement of the  $V_{\text{oc}}$  when fabricating the PVC with one of these polymers as donor and PCBM as acceptor. Furthermore, with increase the number of thiophene units in the main chain, the energy band gaps got from the electrochemical measurement of the polymers change from 2.26 eV (P1), 2.22 eV (P2), 2.16 eV (P3) to 2.15 eV (P4), which are consistent with the  $E_{g,opt}$  determined from absorption measurement.

### Photovoltaic Properties

To investigate the photovoltaic properties of the polymers, the bulk heterojunction solar cells with a structure of ITO/PEDOT-PSS/polymers:PCBM/LiF/Al were fabricated where the polymers were used as donor and PCBM as acceptor. The active layers were prepared by spin coating

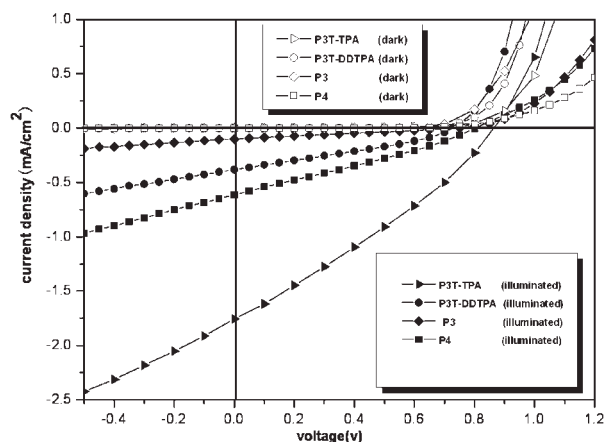


**Figure 6.** Current–voltage characteristics of polymer photovoltaic cells based on P3T-TPA, P3T-DDTPA, P3, P4, and PCBM blend system in the dark and under illumination of  $100 \text{ mW}/\text{cm}^2$  white light.



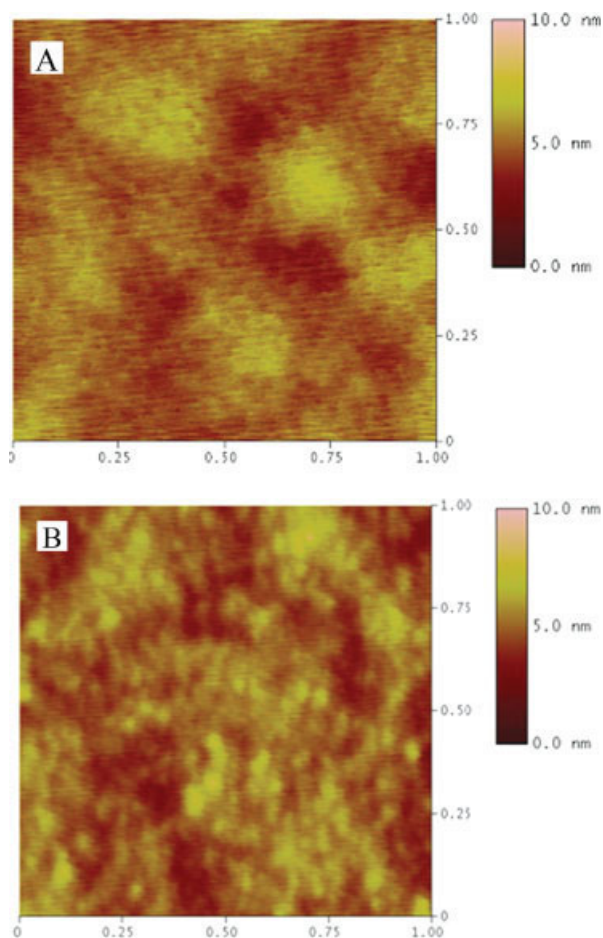


**Figure 7.** AFM images showing the surface morphology of the blend films of (A) P3T-TPA/PCBM (w/w, 1:1); (B) P3T-DDTPA/PCBM (w/w, 1:1); the blend films were spin-coated from their chlorobenzene solutions.

polymers and PCBM in chlorobenzene blend solution with a weight ratio of 1:1.

Figure 6 shows the current-density ( $J$ ) versus voltage ( $V$ ) curves of the polymers PVCs in the dark and under white light illumination at an intensity of  $100 \text{ mW/cm}^2$ . The P3T-TPA device performance shows an open circuit voltage ( $V_{oc}$ ) of 0.87 V, short circuit current ( $J_{sc}$ ) of  $1.76 \text{ mA/cm}^2$ , fill factor (FF) of 0.29, and a PCE of 0.45%, while the P3T-DDTPA device exhibits lower  $V_{oc}$  (0.72 V), higher FF (0.32), but much lower  $J_{sc}$  ( $0.38 \text{ mA/cm}^2$ ), leading to the PCE 0.09%. The low  $J_{sc}$  of both homopolymers is caused by the bad aggregated configuration in solid state which leads to the mismatch of the absorption with the solar spectrum. The bad aggregated configuration is further proved by the AFM images of P3T-TPA/PCBM and P3T-DDTPA/

PCBM blend films (shown in Fig. 7). It is obvious that the AFM image of P3T-TPA/PCBM blend film reveals a roughness with root mean square (RMS) 0.65 nm and slight aggregation. However, the AFM image of P3T-DDTPA/PCBM blend film shows larger roughness (RMS 0.9 nm) and obvious aggregation. The varying degrees of aggregation are also consistent with the values of  $J_{sc}$  (the more obvious aggregation formed the lower  $J_{sc}$  obtained). On the other hand, the decreased  $J_{sc}$  of P3T-DDTPA with long alkoxy compared to P3T-TPA may be also caused by the reduced charge transport capabilities due to the less dense packing of the polymer chains.<sup>41</sup> The  $J_{sc}$  of copolymer (P1, P2, P3) devices decreased to  $0.08 \text{ mA/cm}^2$  (P1),  $0.12 \text{ mA/cm}^2$  (P2),  $0.10 \text{ mA/cm}^2$  (P3) compared to P3T-DDTPA device result from the random copolymerization and low molecular weight (6300–8200 g/mol) and the relatively low carrier mobility.<sup>42–44</sup> The P4 device obtains much higher  $J_{sc}$  ( $0.61 \text{ mA/cm}^2$ ) than the other three copolymers is attributed to the broader absorption and higher regioregularity. Furthermore, all the PVCs obtained promising  $V_{oc}$  in the range of 0.72–0.87 V, which are much higher than the  $V_{oc}$  reported for P3HT:PCBM blends<sup>45</sup> because of the relative low HOMO level of the polymers. The photovoltaic parameters are summarized in Table 3.

P3T-TPA gave the best results with the PCE of 0.45%. We note here that this high efficiency is obtained due to the high  $J_{sc}$  and  $V_{oc}$ . For the copolymers, with the increase of HT units from P1 to P4, the PCE of copolymer devices gradually increased, owing to the reduce disorder degree of copolymerization and broader absorption. Much better efficiencies could be expected by optimizing the polymer/PCBM blend ratio, device configurations, and the morphology of the active layer in PVCs.

**Table 3.** Photovoltaic Characteristics of the Polymers

	$V_{oc}$ (V)	$J_{sc}$ ( $\text{mA/cm}^2$ )	FF	PCE (%)
P3T-TPA	0.87	1.76	0.29	0.45
P3T-DDTPA	0.72	0.38	0.32	0.086
P1	0.71	0.08	0.24	0.011
P2	0.74	0.12	0.25	0.013
P3	0.74	0.10	0.25	0.019
P4	0.80	0.61	0.29	0.142



## CONCLUSIONS

We have synthesized a series of novel PTs derivatives containing TPA as side chains by GRIM method. The absorption spectra of the polymers display that red-shifted and broader absorption were obtained by increasing HT units in the main chain of the polymers. The PL spectra of the polymers revealed that the increase of thiophene units in the main chain enhanced the conjugated length and extended  $\pi$ -delocalized system of the polymers. And the intramolecular energy transfer occurred by introducing dialkoxy-substituted TPA on the side chain of the polymers. Electrochemical characterizations showed that PT containing TPA moiety as side chain possessed relatively higher oxidation potential and lower HOMO level than other PT derivatives, which is benefit for the air-stability and the increase of  $V_{oc}$ , respectively. Bulk heterojunction PVCs with the configuration of ITO/PEDOT:PSS/polymers:PCBM (1:1, w/w)/Al were fabricated. Promising  $V_{oc}$  up to 0.87 V could be obtained. The maximum PCE of devices based on P3T-TPA reached 0.45%. These results indicated that PTs containing TPA as side conjugated chain are very attractive materials for PVC applications. Further improvements could be expected for the PVCs based on these polymers by optimizing the polymer/PCBM ratio, device structure, as well as the morphology of the active layer.

This work was supported by the National Natural Science Foundation of China (Grant No. 50673035), the Program for Changjiang Scholars and Innovative Research Team in University (Grant No. IRT0422), Plan for New Century Excellent Talents in Universities of China Ministry of Education, the Research Project of Jilin Province (Grant No. 20060702), the Research Project of Changchun City (Grant No. 06GH03), and the Science Fund of State Key Laboratory of Polymer Physics and Chemistry (Changchun Institute of Applied Chemistry).

## REFERENCES AND NOTES

- Heeger, A. J. *Angew Chem Int Ed Engl* 2001, 40, 2591–2611.
- Liao, L.; Cirpan, A.; Chu, Q.; Karase, F. E.; Pang, Y. *J Polym Sci Part A: Polym Chem* 2007, 45, 2048–2058.
- Yu, G.; Gao, J.; Hummelen, J. C.; Wudl, F.; Heeger, A. J. *Science* 1995, 270, 1789–1791.
- Zhou, E. J.; Tan, Z. A.; He, Y. J.; Yang, C. H.; Li, Y. F. *J Polym Sci Part A: Polym Chem* 2007, 45, 629–638.
- Dang, T. T. M.; Park, S.-J.; Park, J.-W.; Chung, D.-S.; Park, C. E.; Kim, Y.-H.; Kwon, S.-K. *J Polym Sci Part A: Polym Chem* 2007, 45, 5277–5284.
- Lim, E.; Kim, Y. M.; Lee, J.-I.; Jung, B.-J.; Cho, N. S.; Lee, J.; Do, L.-M.; Shim, H.-K. *J Polym Sci Part A: Polym Chem* 2006, 44, 4709–4721.
- Shin, W. S.; Kim, S. C.; Lee, S.-J.; Jeon, H.-S.; Kim, M.-K.; Naidu, B. V. K.; Jin, S.-H.; Lee, J.-K.; Lee, J. W.; Gal, Y.-S. *J Polym Sci Part A: Polym Chem* 2007, 45, 1394–1402.
- Reyes-Reyes, M.; Kim, K.; Carroll, D. L. *Appl Phys Lett* 2005, 87, 83506.
- Kim, J. Y.; Kim, S. H.; Lee, H. H.; Lee, K. W.; Gong, M. X.; Heeger, A. J. *Adv Mater* 2006, 18, 572–576.
- Ma, W. L.; Yang, C. Y.; Gong, X.; Lee, K.; Heeger, A. J. *Adv Funct Mater* 2005, 15, 1617–1622.
- Hou, J. H.; Tan, Z. A.; He, Y. J.; Yang, C. H.; Li, Y. F. *Macromolecules* 2006, 39, 4657–4662.
- Hou, J. H.; Tan, Z. A.; Yan, Y.; He, Y. J.; Yang, C. H.; Li, Y. F. *J Am Chem Soc* 2006, 128, 4911–4916.
- Shi, C. J.; Yao, Y.; Yang, Y.; Pei, Q. B. *J Am Chem Soc* 2006, 128, 8980–8986.
- Zhang, F. L.; Johansson, M.; Andersson, M. R.; Hummelen, J. C.; Inganäs, O. *Synth Met* 2003, 137, 1401–1402.
- Cheng, K.-F.; Liu, C.-L.; Chen, W.-C. *J Polym Sci Part A: Polym Chem* 2007, 45, 5872–5883.
- Andersson, M. R.; Thomas, Mammo, O. W.; Svensson, M.; Theander, M.; Inganäs, O. *J Mater Chem* 1999, 9, 1933–1940.
- Perzon, E.; Wang, X. J.; Admassie, S.; Inganäs, O.; Andersson, M. R. *Polymer* 2006, 47, 4261–4268.
- Brabec, C. J.; Sariciftci, N. S.; Hummelen, J. C. *Adv Funct Mater* 2001, 11, 15–26.
- Shaheen, S. E.; Brabec, C. J.; Sariciftci, N. S.; Padinger, F.; Fromerz, T.; Hummelen, J. C. *Appl Phys Lett* 2001, 78, 841–843.
- Kuo, C.-H.; Cheng, W.-K.; Lin, K.-R.; Leung, M.-K.; Hsieh, K.-H. *J Polym Sci Part A: Polym Chem* 2007, 45, 4504–4513.
- Lee, S. K.; Ahn, T.; Cho, N. S.; Lee, J.-I.; Jung, Y. K.; Lee, J.; Shim, H. K. *J Polym Sci Part A: Polym Chem* 2007, 45, 1199–1209.
- Huo, L. J.; He, C.; Han, M. F.; Zhou, E. J.; Li, Y. F. *J Polym Sci Part A: Polym Chem* 2007, 45, 3861–3871.
- Roquet, S.; Cravino, A.; Leriche, P.; Aleveque, O.; Frere, P.; Roncali, J. *J Am Chem Soc* 2006, 128, 3459–3466.
- Tamao, K.; Kodama, S.; Nakajima, I.; Kumada, M. *Tetrahedron* 1982, 38, 3347–3354.
- Loewe, R. S.; Khersonsky, S. K.; McCullough, R. D. *Adv Mater* 1999, 11, 250–253.

26. Loewe, R. S.; McCullough, R. D. *Polym Prepr* 1999, 40, 852–853.
27. Sheina, E. E.; Khersonsky, S. M.; Jones, E. G.; McCullough, R. D. *Chem Mater* 2005, 17, 3317–3319.
28. Yang, Z.; Hu, B.; Karasz, F. E. *Macromolecules* 1995, 28, 6151–6154.
29. Barberis, V. P.; Mikroyannidis, J. A. *J Polym Sci Part A: Polym Chem* 2006, 44, 3556–3566.
30. Mallegol, T.; Gmouh, S.; Meziane, M. A. A.; Mongin, O. *Synthesis* 2005, 11, 1771–1774.
31. Xia, H. J.; He, J. T.; Peng, P.; Zhou, Y. H.; Li, Y. W.; Tian, W. J. *Tetrahedron Lett* 2007, 48, 5877–5881.
32. Zhou, E. J.; He, C.; Tan, Z. A.; Yang, C. H.; Li, Y. F. *J Polym Sci Part A: Polym Chem* 2006, 44, 4916–4922.
33. Loewe, R. S.; Ewbank, P. C.; Liu, J. S.; Zhai, L.; McCullough, R. D. *Macromolecules* 2001, 34, 4324–4333.
34. Sheina, E. E.; Liu, J. S.; Iovu, M. C.; Laird, D. W.; McCullough, R. D. *Macromolecules* 2004, 37, 3526–3528.
35. Hiorns, R. C.; Khoukh, A.; Gourdet, B.; Dagron-Lartigau, C. *Polym Int* 2006, 55, 608–620.
36. Iraqi, A.; Barker, G. W. *J Mater Chem* 1998, 8, 25–29.
37. Wan, J. H.; Feng, J. C.; Wen, G. A.; Wei, W.; Fan, Q. L.; Wang, C. M.; Wang, H. Y.; Zhu, R.; Yuan, X. D.; Huang, C. H.; Huang, W. J. *J Org Chem* 2006, 71, 2565–2571.
38. Pommerehne, J.; Vestweber, H.; Guss, W.; Mahrt, R. F.; Bäessler, H.; Porsch, M.; Daub, J. *Adv Mater* 1995, 7, 551–554.
39. Zhou, Y. H.; Peng, P.; Han, L.; Tian, W. J. *Synth Met* 2007, 157, 502–507.
40. Barbarella, G.; Favaretto, L.; Sotgiu, G.; Zambianchi, M.; Arbizzani, G.; Bongini, A.; Mastragostino, M. *Chem Mater* 1999, 11, 2533–2541.
41. Tang, W. H.; Kietzke, T.; Vemulamada, P.; Chen, Z. K. *J Polym Sci Part A: Polym Chem* 2007, 45, 5266–5276.
42. Hou, J. H.; Huo, L. J.; He, C.; Yang, C. H.; Li, Y. F. *Macromolecules* 2006, 39, 594–603.
43. Schilinsky, P.; Asawapirom, U.; Scherf, U.; Biele, M.; Brabec, C. J. *Chem Mater* 2005, 17, 2175–2180.
44. Hiorns, R. C.; de Bettignies, R.; Leroy, J.; Bailly, S.; Firon, M.; Sentein, C.; Khoukh, A.; Preud'homme, H.; Dagron-Lartigau, C. *Adv Funct Mater* 2006, 16, 2263–2273.
45. Li, G.; Shrotriya, V.; Huang, J. S.; Yao, Y.; Moriarty, T.; Emery, K.; Yang, Y. *Nat Mater* 2005, 4, 864–869.